

A New Molecular Imprinting-Based Mass-Sensitive Sensor for Real-Time Detection of 17 β -Estradiol from Aqueous Solution

Erdoğan Özgür,¹ Erku Yılmaz,¹ Gülsu Şener,^{1,2} Lokman Uzun,¹ Ridvan Say,³ and Adil Denizli¹

¹ Department of Chemistry, Biochemistry Division, Hacettepe University, Ankara, Turkey; denizli@hacettepe.edu.tr (for correspondence)

² Nanotechnology and Nanomedicine Division, Hacettepe University, Ankara, Turkey

³ Department of Chemistry, Anadolu University, Eskişehir, Turkey

Published online in Wiley Online Library (wileyonlinelibrary.com). DOI 10.1002/ep.11718

The 17 β -estradiol (E2), natural steroid hormone, is one of the most potent endocrine disrupting compounds even at ng L⁻¹ levels. Its rapid, selective and sensitive detection is intensively required. In this study, quartz crystal microbalance (QCM) sensor was prepared for real-time monitoring of E2 in water samples, through the attachment of E2 imprinted nanoparticles, synthesized by mini-emulsion polymerization, on the gold surface of QCM sensor. QCM sensor surface was characterized by atomic force microscopy (AFM), ellipsometer, and contact angle measurements. The specificity of the QCM nanosensor was shown by competitive adsorption of E2, stigmaterol and cholesterol. The results showed that QCM nanosensor has high selectivity and sensitivity for E2 even in a wide range of 3.67 nM–3.67 μ M. The detection and quantification limits were calculated as 613 fM and 2.04 pM, respectively. According to the results, the proposed molecular imprinted QCM nanosensor is promising cost-friendly alternative for quantification of E2 from ground water. © 2012 American Institute of Chemical Engineers Environ Prog, 00: 000–000, 2012

Keywords: 17 β -estradiol (E2), molecular imprinted nanosensor, quartz crystal microbalance, micropollutants, endocrine disruptors

INTRODUCTION

Endocrine disrupting chemicals (EDCs) are defined as exogenous substances that alter function(s) of the endocrine system and consequently cause adverse effects on growth, metabolism and reproduction, in an intact organism, or (sub)populations, even at low concentrations [1, 2]. A wide range of substances are known as EDCs like estrogens, progestrogens and phytoestrogens, synthetic estrogens, a wide variety of organic pollutants, pesticides and surfactants [3]. Therefore, EDCs were included in the list of emerging contaminants by the European Union [4]. Among them, steroid estrogens include estrone (E1), 17 β -estradiol (E2), estriol (E3), and 17 β -ethynylestradiol (EE2) are the most potent endocrine disruptors [5]. E2 excreted by humans and animals, is one of the most important steroid estrogenic hormones that influence the development and maintenance of female sexual characteristics of many species [6, 7]. E2 concentration

of 1–10 ng L⁻¹ causes feminization of male fish and E2 concentration of 1.0 ng L⁻¹ vitellogenin (a biomarker of estrogenic contamination in the aquatic environment) production in male fish [8, 9]. However, inappropriate uses can cause negative effects primarily through endocrine disruption such as increasing rates of breast cancer in women and in wildlife; hermaphroditism and decreased fertility [3, 10]. This estrogenic hormone is used also in human health and animal farming practices [11, 12]. For the determination of E2, many methods such as enzyme-linked immunosorbent assay (ELISA) [13], chromatographic techniques [14], radioimmunoassay (RIA), microplate chemiluminescence immunoassay [7], electrochemical sensor [15], and measuring the change in fluorescence emission intensity [16] have been reported. The increasing use of pharmaceuticals, chemicals, accidental spills, and releases of some estrogenic compounds causes the load of estrogenic substances in the aquatic environment [17]. Therefore, it is necessary to detect and quantify these compounds to prevent adverse effects on human and wildlife.

Quartz crystal microbalance (QCM), high-resolution mass sensing technique, measures changes in mass on oscillating quartz crystal surface by measuring changes in oscillation frequency of crystal in real time [18]. The mass sensing technique provides label-free, selective, simple, and stable detection methods [21]. QCM technique have already been used in the detection of clinical targets [20], environmental contaminants [21], marker of genetic diseases [22], determination of oxidative stress [23, 24], quantification of proteins [25], and bimolecular interactions [26]. Molecular imprinted particles (MIPs) were used to obtain selective polymer layer on the surface of QCM sensor. Molecular imprinting technique, based on molecular recognition, provides the polymerization of synthetic materials which have specific binding sites and geometric shapes in their high crosslinked structure for the interested molecules called as target molecules [25–27].

In this study, we aimed to prepare QCM nanosensor using E2 imprinted nanoparticles. The main steps of this study are the synthesis of E2 imprinted poly(2-hydroxyethyl methacrylate-*N*-methacryloyl-*l*-tyrosine methylester) (PHEMAT) nanoparticles and attaching them onto QCM sensor surface. E2 solutions with different concentrations were applied to QCM system to investigate the detection dynamics and the effective parameters were calculated.

EXPERIMENTAL

Materials

The 17 β -estradiol (E2) (E 8875-56), *L*-tyrosine methylester, poly(vinyl alcohol) (PVA), sodium dodecyl sulfate (SDS), ammonium persulfate, sodium bicarbonate, sodium bisulfite, and potassium bromide (FTIR grade) were obtained from Sigma Chemical (St. Louis, USA). Ethylene glycol dimethacrylate (EDMA), 2-hydroxyethyl methacrylate (HEMA), and absolute methanol were purchased from Fluka A.G. (Buchs, Switzerland). HEMA and EDMA were distilled under reduced pressure in the presence of hydroquinone inhibitor and stored at 4°C until use. All other chemicals were reagent grade and purchased from Merck A.G. (Darmstadt, Germany). Specific functional comonomer, *N*-methacryloyl-*L*-tyrosine methylester (MAT), was supplied from Nanoreg (Ankara, Turkey).

Preparation of E2 Imprinted PHEMAT Nanoparticles

E2 imprinted PHEMAT nanoparticles were prepared by two phase miniemulsion polymerization method [25]. The first aqueous phase was prepared by dissolving of PVA (200 mg), SDS (30 mg), and sodium bicarbonate (25 mg) in 10 mL deionized water. The second phase was prepared by dissolving of PVA (100 mg) and SDS (100 mg) in 200 mL of deionized water. The monomer phase was prepared by using MAT (100 μ L), HEMA (0.7 mL), and EDMA (1.4 mL). The monomer phase was slowly added to the first aqueous phase. To obtain miniemulsion, the mixture was homogenized at 25,000 rpm by a homogenizer (T10, Ika Labortechnik, Germany). After homogenization, the template molecule (E2, 200 μ mol) was added to miniemulsion and the mixture was stirred to obtain effectively interacted monomer-template pre-polymerization complex for 2 h. Then, the mixture was slowly added to the second aqueous phase while the phase has been stirring in a sealed-cylindrical polymerization reactor (250 mL). The reactor was magnetically stirred at 300 rpm (Radleys Carousel 6, UK). The polymerization mixture was slowly heated to 40°C, polymerization temperature. After that, nitrogen gas was bubbled through the solution for removing dissolved oxygen for 5 min. Then, initiators, sodium bisulfite (125 mg) and ammonium persulfate (125 mg), were added into the solution. Polymerization was continued at 40°C for 24 h. The E2 imprinted nanoparticles were washed with water and water/ethyl alcohol mixtures, to remove unreacted monomers, surfactant and initiators. For each washing step, the solution was centrifuged at 30,000 rpm for 30 min (Allegra-64R Beckman Coulter, USA); then, the nanoparticles were dispersed in fresh washing solution. After last washing step, the E2 imprinted nanoparticles were dispersed in deionized water containing 0.3% sodium azide and stored at 4°C. The nonimprinted nanoparticles (NIP) were synthesized by the same experimental procedure without using E2 as template.

Characterization of E2 Imprinted PHEMAT Nanoparticles

Characterization studies of the nanoparticles were carried out by Zetasizer (NanoS, Malvern Instruments, London, UK) and FTIR-ATR spectrophotometer. In zeta-size measurement; for data analysis, density and refraction index of deionized water were used as 0.88 and 1.33 mPa s⁻¹, respectively. Light scattering was done at incidence angle 90° and 25°. Light scattering signal was calculated as nanoparticle number per second. For FTIR-ATR measurement; E2 imprinted nanoparticles were put in a sample holder of FTIR-ATR spectrophotometer (Thermo Fisher Scientific, Nicolet iS10, Waltham, MA), airborne moisture and CO₂ were removed from the sample by passing N₂ for 10 min and total light reflection

from surface was measured in the wavenumber range of 400–4000 cm⁻¹ at 2 cm⁻¹ resolution. Baseline correction was done due to Ge window.

Preparation of E2 Imprinted QCM Nanosensor

Gold surface of QCM sensor was cleaned in hot piranha solution (7:3 H₂SO₄: H₂O₂, v/v) for 1–2 min, before attachment of E2 imprinted particles onto gold surface. Then, it was rinsed with pure ethyl alcohol, deionized (DI) water, and dried in vacuum oven (200 mmHg, 37°C) for 3 h. To prepare the gold surface of QCM sensor, E2 imprinted particles included solution (5 μ L) were dropped on the gold surface and dried at 37°C for 6 h. Then, E2 imprinted QCM nanosensor was washed with both water and ethyl alcohol and dried with nitrogen gas under vacuum (200 mmHg, 37°C).

Template Removal from Nanosensor

Its expected that functional monomer MAT interacts with E2 through H-bonds and hydrophobic interactions through aromatic ring. To break these interactions, ethylene glycol solution (20%, v/v) was used as a desorption agent. Removal of E2 was carried out via continuous and batch systems, respectively. E2 imprinted QCM nanosensor was immersed into desorption solution (20 mL). The nanosensor was shaken in bath (200 rpm) at room temperature. After E2 removal, the nanosensor was washed with deionized water and dried with nitrogen gas under vacuum (200 mmHg, 25°C).

Characterization of E2 Imprinted QCM Nanosensor

Prepared QCM sensor surface was characterized with atomic force microscopy (AFM), ellipsometer and contact angle measurements. AFM observations were carried out by using AFM (Nanomagnetics Instruments, Oxford, UK) in tapping mode. E2 imprinted QCM nanosensor was attached on sample holder by using double-side carbon strip. Observation study was carried out via tapping mode in air atmosphere. Applied experimental parameters were oscillation frequency (341.30 kHz), vibration amplitude (1 V_{RMS}) and free vibration amplitude (2 V_{RMS}). Samples were scanned with 2 μ m s⁻¹ scanning rate and 256 \times 256 pixels resolution to obtain view of 2 \times 2 μ m² area. Ellipsometer measurement was carried out by an auto-nulling imaging ellipsometer (Nanofilm EP3, Germany). All thickness measurements have been performed at a wavelength of 532 nm with an angle of incidence of 72°. In the layer thickness analysis, a four-zone auto-nulling procedure integrating over a sample area of \sim 50 \times 50 μ m² followed by a fitting algorithm has been performed. Measurement was carried out as triplicate on six different points of sensor surface and the results were reported as mean value of the measurements with standard deviations. Contact angle measurements were determined with Krüss DSA100 (Hamburg, Germany) instrument. Contact angle of gold sensor surface was measured with Sessile Drop method by dropping 1 water drop. Ten separate photos were taken from the different parts of sensor surfaces and contact angle values were measured for each drop. Measured contact angle values were obtained as the left contact angle, the angles from the left contact point of the droplet with solid and right contact angle from the right contact point. In addition, average contact angle values were obtained from the average of two values. Contact angle values for the gold surfaces of the QCM sensor were the average of the 10 measurements.

Evaluation of E2 Imprinted QCM Nanosensor Response

The real time detection of E2 from aqueous solution was performed by using a QCM system (RQCM, INFICON

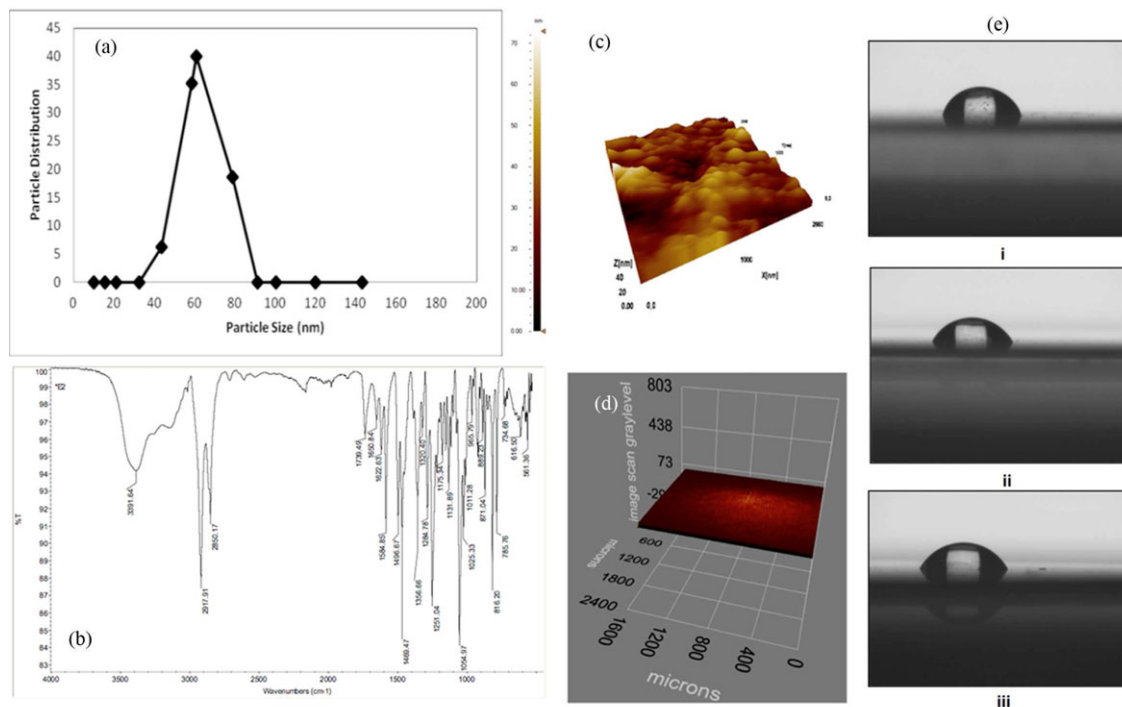


Figure 1. Characterization of E2 imprinted PHEMAT particles and sensor. (a) Zeta-size measurements; (b) FTIR-ATR spectrum; (c) AFM images of E2 imprinted QCM sensor, (d) Ellipsometer images of E2 imprinted QCM sensor, and (e) Contact angles measurements of imprinted (i), nonimprinted (ii) QCM nanosensor and nonmodified (iii) QCM nanosensor. [Color figure can be viewed in the online issue, which is available at [wileyonlinelibrary.com](http://www.wileyonlinelibrary.com).]

Acquires Maxtek, NY). The kinetic and affinity studies were determined by using E2 solutions with different concentrations in the range of 3.67 nM–3.67 pM. First, the QCM nanosensor was washed with deionized water (50 mL, 1.0 mL min⁻¹ flow-rate) and equilibration buffer (pH: 11.0, carbonate, 50 mL, 2.0 mL min⁻¹ flow-rate) to obtain the steady resonance frequency (f_0). After that, the E2 solutions in different concentration range 3.67 nM–3.67 pM in carbonate buffer were applied to QCM system (5 mL and 1.0 mL min⁻¹ flow-rate). Monitoring of the QCM nanosensor frequency maintained until it became stable (150 min, approximately). Then, desorption studies were performed by using 10 mL of ethylene glycol solution (20%, v/v) with 1.0 mL min⁻¹ flow-rate. After desorption, the E2 imprinted QCM nanosensor was washed with deionized water and equilibration buffer. These steps were cycled for each E2 solution.

RESULTS AND DISCUSSION

Preparation and Characterization of E2 Imprinted QCM Nanosensor

Preparation of E2 imprinted nanoparticles was carried out using a miniemulsion polymerization procedure [25]. Average size and size distribution of the nanoparticles were determined by zeta-sizer. E2 imprinted nanoparticles have average diameter as 65.5 nm with a polydispersity around 0.37 (Figure 1a). The imprinted nanoparticles were also characterized by FTIR-ATR (Figure 1b). In the spectrum, aliphatic –CH band at 2917 cm⁻¹, –OH band about at 3391 cm⁻¹ and carbonyl band at 1739 cm⁻¹ originated from methacrylate structure, were determined. Amide bands of functional monomer, MAT, were determined at 1622 and 1496 cm⁻¹, respectively. C=C–H asymmetric stretching at 3025 cm⁻¹, C=C=C symmetric stretching at 1584 cm⁻¹ and C=C=C

asymmetric stretching at 1469 cm⁻¹ bands of benzene ring were also determined.

For more detailed information about nanoparticle coating, QCM nanosensor surface was characterized by atomic force microscopy (AFM) and ellipsometry. Surface depth determined by AFM measurements of the E2 imprinted QCM nanosensor is about 50 nm (Figure 1c). AFM observation matched the size of nanoparticle as obtained by zeta-sizer measurement. AFM scan over a 2 μm × 2 μm area showed that the nanoparticles were well distributed (almost homogeneously) on the QCM sensor surface. Ellipsometry analysis was also carried out and coherency is seen between AFM and ellipsometer measurements. Surface depth obtained from ellipsometer of E2 imprinted QCM nanosensor is 73 nm (Figure 1d). The thickness measurements and AFM observations indicated that the nanoparticle distribution on nanosensor surface was almost homogeneous.

As seen in contact angle measurements (Figure 1e), contact angle values of nonmodified QCM nanosensor surface, E2 imprinted PHEMAT nanoparticles attached QCM sensor surface and nonimprinted PHEMAT nanoparticles attached QCM sensor surface were 60.73°, 72.95°, and 67.20°, respectively. Increase in surface contact angle showed that hydrophobicity of the surface increased. Hydrophobic character of surface is expected because of the hydrophobic structure of MAT monomer.

Response of E2 Imprinted QCM Nanosensor

E2 imprinted PHEMAT nanoparticles attached QCM nanosensor was tested for the real-time detection of E2 from aqueous solution. Figure 2 shows frequency shifts (Δf) of QCM responding to different concentrations of aqueous E2 solutions in the range of 3.67 nM–3.67 pM. The increasing concentration of E2 in solution caused the increasing

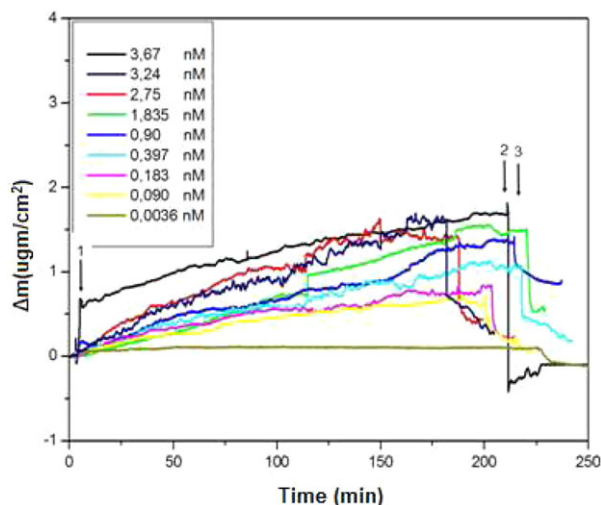


Figure 2. Response of E2 imprinted QCM sensor to different concentrations of aqueous E2 solutions (1) adsorption, (2) desorption, (3) regeneration. [Color figure can be viewed in the online issue, which is available at [wileyonlinelibrary.com](http://www.wileyonlinelibrary.com).]

response of the nanosensor, because Δf depends on the concentration of E2.

Figure 3 shows the relationship between mass shift and E2 concentration. E2 imprinted QCM nanosensor has two different linear regions for aqueous E2 solutions. The results show E2 molecules bound to E2 imprinted nanosensor through two different orientations with high affinity. QCM nanosensor shows a linearity of 92% in the concentration range of 3.67–0.367 nM and a linearity of 87% in the concentration range of 0.183 nM–3.67 pM. The results mainly depend on the spherical structure of imprinted nanoparticles. When imprinted nanoparticles were attached on the nanosensor surface, some of the imprinted cavities were sterically hindered. Therefore, E2 molecules can not reach these cavities as easily as upper cavities; but still have high affinity to them [25].

Equilibrium Analysis

Under pseudo-first order conditions where the free analyte concentration is held constant in the flow cell, the binding can be described by following equation;

$$d\Delta m/dt = k_a C \Delta m_{\max} - (k_a C + k_d) \Delta m \quad (1)$$

where $d\Delta m/dt$ is the rate of change of the QCM signal, Δm and Δm_{\max} are the measured and maximum response signal measured with binding, C is the injected concentration of E2 (nM), k_a is the association rate constant (nM s^{-1}) and k_d is the dissociation rate constant (1/s). The binding constant, K_A , may be calculated as $K_A = k_a/k_d$. At equilibrium, $d\Delta m/dt = 0$ and the equation can be rewritten:

$$\Delta m_{\text{eq}}/C = K_A \Delta m_{\max} - K_A \Delta m_{\text{eq}} \quad (2)$$

Therefore, the steady state association constant K_A can be obtained from a plot of $\Delta m_{\text{eq}}/C$ versus Δm_{eq} and the dissociation constant K_D can be calculated as $1/K_A$.

Equation 1 may be rearranged to give:

$$d\Delta m/dt = k_a C \Delta m_{\max} - (k_a C + k_d) \Delta m \quad (3)$$

Thus a plot of $d\Delta m/dt$ against Δm will theoretically be a straight line with slope $-(k_a C + k_d)$ for interaction-controlled kinetics. The initial binding rate is directly proportional to the analyte concentration and can be used for concentration

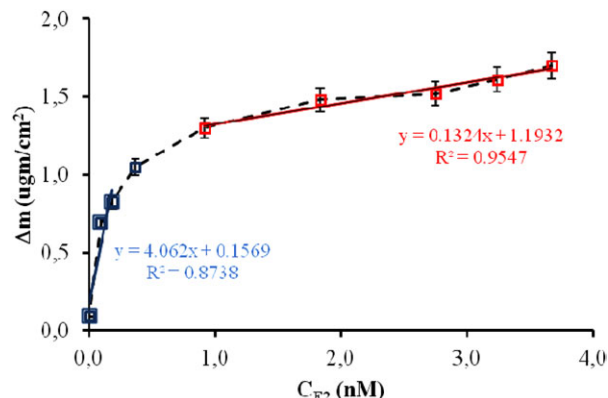


Figure 3. Relationship between concentration and mass change (Δm). [Color figure can be viewed in the online issue, which is available at [wileyonlinelibrary.com](http://www.wileyonlinelibrary.com).]

measurements. If Δm_{\max} is known, both k_a and k_d can be determined from a single association sensorgram. Δm_{\max} is, however, often difficult to determine experimentally, since a high analyte concentration is required to fully saturate the surface. A preferable approach is to measure the association sensorgram at several different analyte concentrations. For analysis of the forward and back rates, a plot of the change in total sensor response ($d\Delta m/dt$) versus Δm gives a value S as the slope that relates the forward and back rates as follows:

$$S = k_a C + k_d \quad (4)$$

A plot of S against C will be a straight line with slope k_a . In theory, the intercept on the ordinate ($C = 0$) give k_d ; in practice, however, this cannot be used as a reliable measure of the dissociation rate constant if $k_a C \gg k_d$. A more accurate way to obtain this value is by direct measurement of the dissociation from saturated binding sites into a buffer solution flow that contains no analyte and the dissociation is quantified by:

$$\ln(\Delta m_o/\Delta m_t) = k_d(t - t_o) \quad (5)$$

where m_o is the initial response level at t_o and m and t represent values obtained along the dissociation curve [28].

Equilibrium Isotherm Models

Adsorption isotherms, as Scatchard, Langmuir, Freundlich, and Langmuir–Freundlich, were used to evaluate adsorption properties.

$$\text{Scatchard} \quad \Delta m_{\text{eq}}/C = K_A(\Delta m_{\max} - \Delta m_{\text{eq}}) \quad (6)$$

$$\text{Langmuir} \quad \Delta m = \{\Delta m_{\max} C / K_D + C\} \quad (7)$$

$$\text{Freundlich} \quad \Delta m = \Delta m_{\max} C^{1/n} \quad (8)$$

$$\text{Langmuir - Freundlich} \quad \Delta m = \{\Delta m_{\max} C^{1/n} / K_D + C^{1/n}\} \quad (9)$$

where K_D is equilibrium dissociation constant and $1/n$ is Freundlich heterogeneity index.

Scatchard, Langmuir, Freundlich, and Langmuir–Freundlich isotherms were applied to experimental data to describe the interaction model between E2 imprinted QCM nanosensor and E2 molecule (Table 1). After applying these isotherm models to the system, it was found that Langmuir isotherm model was the best fitted to the system ($R^2 = 0.998$). The Langmuir model assumes a monomolecular layer on a homogeneous surface. The binding sites have the same adsorption

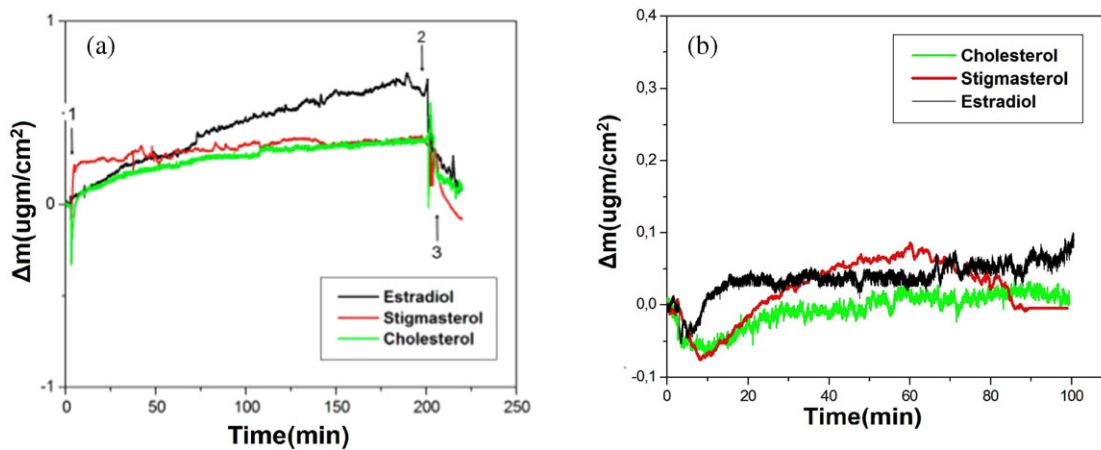


Figure 4. Comparison of selectivity of QCM sensors. The responses of (a) E2 imprinted and (b) nonimprinted QCM sensor. [Color figure can be viewed in the online issue, which is available at [wileyonlinelibrary.com](http://www.wileyonlinelibrary.com).]

Table 1. Kinetic and isotherm parameters

Equilibrium analysis (Scatchard)		Association kinetics analysis	
Δm_{\max} , $\mu\text{g cm}^{-2}$	1.444	k_a , nM s^{-1}	0.0005
K_A , nM	14.135	k_d , 1 s^{-1}	0.0077
K_D , nM^{-1}	0.692	K_A , nM	0.0649
R^2	0.8092	K_D , nM^{-1}	15.40
		R^2	0.9143

Langmuir		Freundlich		Langmuir–Freundlich	
Δm_{\max} , $\mu\text{g cm}^{-2}$	1.239	Δm_{\max} , $\mu\text{g cm}^{-2}$	1.328	Δm_{\max} , $\mu\text{g cm}^{-2}$	1.697
K_D , nM^{-1}	0.04697	$1/n$	0.4198	$1/n$	0.4198
K_A , nM	21.29	R^2	0.928	K_D , nM^{-1}	1.846
R^2	0.998			K_A , nM	0.542
				R^2	0.9817

affinity which are energetically equal without any interaction between the adsorbed molecules and each site can hold only one molecule [29] Δm_{\max} value, calculated by using by Langmuir isotherm model, was very close to the experimental one (1.239 nM). K_A and K_D values were determined as 21.29 nM and 0.0469 nM^{-1} , respectively.

Selectivity of E2 Imprinted QCM Nanosensor

To show the selectivity of the E2 imprinted PHEMAT nanoparticles attached QCM nanosensor, competitive adsorption of E2, stigmaterol and cholesterol was investigated (Figure 4). Stigmaterol and cholesterol are very close to E2 in molecular structures and weights. As seen in the Figure 4, E2 imprinted QCM nanosensor was more selective with respect to the solution of stigmaterol and cholesterol which have the same concentration of 0.090 nM with E2 solution, respectively. Selectivity coefficients (k) and relative selectivity coefficients (k') values are displayed in Table 2. E2 imprinted QCM nanosensor was 2.20 and 2.15 times more selective for E2 than stigmaterol and cholesterol, respectively. The results indicate that E2 imprinted QCM nanosensor have higher adsorption capabilities for E2 than for either stigmaterol or cholesterol, due to selective cavities in the polymer structure. To show the specificity of E2 imprinted QCM nanosensor,

Table 2. Selectivity of E2 imprinted QCM nanosensor

	MIP		NIP		
	Δm	k	Δm	k	k'
Estradiol	0.687	—	0.022	—	—
Stigmaterol	0.312	2.20	0.025	0.88	2.50
Cholesterol	0.320	2.15	0.023	0.95	2.26

Table 3. The values for the limit of detection and the limit of quantification

The limit of detection (LOD)	613 fM
The limit of quantification (LOQ)	2.04 pM

nonimprinted QCM nanosensor was used and the responses of nonimprinted QCM nanosensor to E2, stigmaterol and cholesterol were determined as 0.022, 0.025, and 0.023, respectively. And the result show that E2 imprinted QCM nanosensor was 2.50 and 2.26 times selective with respect to the stigmaterol and cholesterol, respectively.

CONCLUSIONS

As a conclusion, QCM-based sensors are so effective that they allow real time monitoring of adsorbed analyte mass and it is not necessary to label the sample [30]. The integration of MIPs with sensors offers a number of advantages such as long-term storage stability, reusability, resistance to microbial spoilage, and robustness to a range of harsh operating conditions [30, 31]. In the present study, E2 imprinted QCM nanosensor was prepared for the detection of a trace amount of E2 in environmental waters. QCM sensor was prepared by attachment of E2 imprinted PHEMAT nanoparticles on the gold surface of QCM sensor. The obtained values (Table 3) for detection limit, 613 fM, and quantification limit, 2.04 pM, concluded that the proposed molecular imprinted QCM nanosensor is promising cost-friendly alternative for quantification of E2 from ground water with its properties such as low cost, easy preparability and applicability.

LITERATURE CITED

1. WHO/IPCS. (2002). Global assessment of the state-of-the-science of endocrine disruptors. World Health Organization/International Program on Chemical Safety.

WHO/PCS/EDC/02.2. Available at: www.who.int/pcs/emerg_site/edc/global_edc_ch5.pdf

2. Mills, L.J. & Chichester, C. (2005). Review of evidence: Are endocrine disrupting chemicals in the aquatic environment impacting fish populations?, *Science of the Total Environment*, 343, 1–34
3. Farre, M., Kuster, M., Brix, R., Rubio, F., Lopez de Alda, M.J., & Barcelo D. (2007). Comparative study of an estradiol enzyme-linked immunosorbent assay kit, liquid chromatography-tandem mass spectrometry, and ultra performance liquid chromatography-quadrupole time of flight mass spectrometry for part-per-trillion analysis of estrogens in water samples, *Journal of Chromatography A*, 1160, 166–175
4. European Commission Report. (2001). Identification of priority hazardous substances. Stockholm Convention. Brussels, Adonis no. 901019.
5. Khanal, S.K., Xie, B., Thompson, M.L., Sung, S., Ong, S., & Leeuwen J.V. (2006). Fate, transport, and biodegradation of natural estrogens in the environment and engineered systems, *Environmental Science and Technology*, 40, 6537–6546
6. Zhang, Z., Rhind, S.M., Kerr, C., Osprey, M., & Kyle, C.E. (2011). Selective pressurized liquid extraction of estrogenic compounds in soil and analysis by gas chromatography-mass spectrometry, *Analytica Chimica Acta*, 685, 29–35
7. Sun, M., Du, L., Gao, S., Bao, Y., & Wang, S. (2010). Determination of 17 β -estradiol by fluorescence immunoassay with streptavidin-conjugated quantum dots as label, *Steroids*, 75, 400–403
8. Sumpter, J.P. & Jobling, S. (1995). Vitellogenesis as a biomarker of estrogenic contamination in the aquatic environment, *Environmental Health Perspectives*, 103, 173–178
9. Purdom, C.E., Hardiman, P.A., Bye, V.J., Eno, N.C., Tyler C.R., & Sumpter, J.P. (1994). Estrogenic effects of effluents from sewage treatment works, *Chemistry and Ecology*, 8, 275–285
10. Moran, C., Quirke, J.F., Prendiville, D.J., Bourke, S., & Roche, J.F. (1991). The effect of estradiol, trenbolone acetate, or zeranol on growth rate, mammary development, carcass traits, and plasma estradiol concentrations of beef heifers, *Journal of Animal Science*, 69, 4249–4258
11. Witorsch, R.J. (2002). Endocrine disruptors: can biological effects and environmental risks be predicted?, *Regulatory Toxicology and Pharmacology*, 36, 118–130
12. Wolf, O.T. & Kirschbaum, C. (2002). Endogenous estradiol and testosterone levels are associated with cognitive performance in older women and men, *Hormones and Behavior*, 41, 259–266
13. Valentini, F., Compagnone, D., & Gentili, A. (2002). An electrochemical ELISA procedure for the screening of 17 β -estradiol in urban waste waters, *Analyst*, 127, 1333–1337
14. Kuch, H. M. & Ballschmitter, K. (2000). Determination of endogenous estrogens in effluents from sewage treatment plants at the level ng/L- level, *Fresenius' Journal of Analytical Chemistry*, 366, 392–395
15. Yuana, L., Zhanga, J., Zhoua, P., Chena, J., Wanga, R., Wena, T., Li, Y., Zhoua, X., Jianga, H. (2011). Electrochemical sensor based on molecularly imprinted membranes at platinum nanoparticles-modified electrode for determination of 17 β -estradiol, *Biosensors and Bioelectronics*, 29, 29–33
16. Yu Yang, Y. and Lai, E.P. C. (2011). Optimization of molecularly imprinted polymer method for rapid screening of 17 β - estradiol in water by fluorescence quenching, *International Journal of Analytical Chemistry*, 2011, 8.
17. Falconer, I.R., Chapman, H.F., Moore, M.R., & Ranmuthugala, G. (2006). Endocrine-disrupting compounds: A review of their challenge to sustainable and safe water supply and water reuse, *Environmental Toxicology*, 21, 181–191
18. Marx, K.A. (2003). Quartz crystal microbalance: A useful tool for studying thin polymer films and complex biomolecular systems at the solution-surface interface, *Bio-macromolecules*, 4, 1099–1120
19. Guilherme, N.M., da-Silva, F.A.C., & Tome, B. (2009). Acoustic wave biosensors: Physical models and biological applications of quartz crystal microbalance, *Trends in Biotechnology*, 27, 689–697
20. Kurosawa, S., Park, J.W., Aizawa, H., Wakida, S., Tao, H., & Ishihara, K. (2006). Quartz crystal microbalance immunosensors for environmental monitoring, *Biosensors and Bioelectronics*, 22, 473–481
21. Mao, Y.A., Wei, W.Z., Zhang, S.F., & Zeng, G.M. (2002). Monitoring, and estimation of kinetic data, by piezoelectric impedance analysis, of the binding of the anticancer drug mitoxantrone to surface-immobilized DNA, *Analytical and Bioanalytical Chemistry*, 373, 215–221
22. Kurosawa, S., Park, J.W., Aizawa, H., Wakida, S., Tao, H., & Ishihara, K. (2006). Quartz crystal microbalance immunosensors for environmental monitoring, *Biosensors and Bioelectronics*, 22, 473–481
23. Minunni, A., Mascini, M., & Tombelli, S. (2006). Analytical applications of QCM-based nucleic acid biosensors, *Piezoelectric Sensors*, 5, 211–237
24. Say, R., Gultekin, A., Özcan, A.A., Denizli, A., & Ersöz, A. (2009). Preparation of new molecularly imprinted quartz crystal microbalance hybride sensor system for 8-hydroxy-2'-deoxyguanosine determination, *Analytica Chimica Acta*, 640, 82–86
25. Ersöz, A., Diltemiz, S.E., Özcan, A.A., Denizli, A., & Say, R. (2009). 8-OHdG sensing with MIP based solid phase extraction and QCM technique, *Sensors and Actuators B*, 137, 7–11
26. Şener, G., Özgür, E., Yılmaz, E., Uzun, L., Say, R., & Denizli, A. (2010). Quartz crystal microbalance based nanosensor for lysozyme detection with lysozyme imprinted nanoparticles, *Biosensors and Bioelectronics*, 26, 815–821
27. Svedhem, S., Dahlborg, D., Ekeröth, J., Kelly, J., Höök, F., & Gold, J. (2003). In situ peptide-modified supported lipid bilayers for controlled cell attachment, *Langmuir*, 19, 6730–6736
28. Wulff, G. (1986). Molecular recognition in polymers prepared by imprinting with templates, *ACS Symposium Series*, American Chemical Society, 308, 186–230
29. Lin, L.P., Huang, L.S., Lin, C.W., Lee, C.K., Chen, J.L., Hsu, S.M., & Lin, S. (2005). Determination of binding constant of DNA-binding drug to target DNA by surface plasmon resonance biosensor technology, *Current Drug Targets*, 5, 61–72
30. Papageorgiou, S.K., Katsaros, F.K., Kouvelos, E.P., & Kanellopoulos, N.K. (2009). Prediction of binary adsorption isotherms of Cu²⁺, Cd²⁺ and Pb²⁺ on calcium alginate beads from single adsorption data, *Journal of Hazardous Materials*, 162, 1347–1354
31. Whitcombe, J.M., Chianella, I., Larcombe, L., Piletsky, S.A., Noble, J., Porter, R., & Horgan, A. (2011). The rational development of molecularly imprinted polymer-based sensors for protein detection, *Chemical Society Reviews*, 40, 1547–1571
32. Şener, G., Uzun, L., Say, R., & Denizli, A. (2011). Use of molecular imprinted nanoparticles as biorecognition element on surface plasmon resonance sensor, *Sensors and Actuators B*, 160, 791–799